

Measurement of diameter of metal cylinders using a sinusoidally vibrating interference pattern

Jinhuan Li, Osami Sasaki*, and Takamasa Suzuki*
Graduate School of Science and Technology, Faculty of Engineering*,
Niigata University, Niigata-shi 950-2181, Japan

ABSTRACT

A method for measuring diameters of metal cylinders is proposed. In this method a sinusoidally vibrating interference pattern (SVIP) of 100 μm -period is used to generate an exact spatial scale along x-axis. Detection of the amplitude and the phase of the SVIP are carried out easily and exactly with sinusoidal phase-modulating interferometry. First, phase values of the SVIP on the pixels of the CCD image sensor are measured as the exact scale along the x-axis. Next, an image of the end-points of the cylinder surface is formed by extracting lights from the end-points of the cylinder. The phase of the SVIP on the end-point of the cylinder appears at a position where the amplitude of the image has maximum value along the x-axis. The x-coordinate of the end-point of the metal cylinder is calculated from the phase value of the end-point and the exact scale. The diameter is obtained from the x-coordinates of the two end-points. Metal cylinders of 9mm and 8mm-diameters are measured with an error of about $\pm 2\mu\text{m}$.

Keywords: diameter measurement, interference pattern, sinusoidal phase-modulation, optical imaging.

1. INTRODUCTION

Optical diffraction methods have been used to measure external diameters.^{1, 2} These methods are suitable to measure the diameters of wires and thin cylinders whose maximum diameters are limited to hundreds micrometers. For measuring large external diameters, shadow techniques are used.^{3, 4} A light beam is translated across a cylinder at a steady speed and detect positions of the two edge shadows of the cylinder to measure the external diameter. This method needs mechanical scanning of the laser beam and the measuring time becomes long when the cylinder is very thick. To remove the scanning, a collimated light beam is incident on the cylinder to form the two edge shadows in a moment. When the edge shadows or intensity distribution of the sectional image of the cylinder are detected with a CCD image sensor, the positions of the two edges of the cylinder in the image are determined by using the pixel positions of the CCD image sensor. Accuracy and region of the diameter measurement depend on the pixel size and number of the pixels of the CCD. To obtain a high accuracy a large magnification of the sectional image is required, which decreases the size of the measurement region. In this paper, in order to obtain both a high accuracy and a wide region of the measurement, a sinusoidally vibrating interference pattern (SVIP)^{5, 6} of period P is used as an exact spatial scale along x-axis. The SVIP is illuminated on the cylinder surface. Lights from the end-points of the cylinder surface are extracted by spatial frequency filtering in an imaging system so that the cross sectional image of the cylinder is formed. On the image plane a sinusoidal phase-modulated signal owing to the SVIP is detected with a two-dimension CCD image sensor. The phase of the signal detected at the measuring point where the amplitude of the signal has a maximum along the x-axis provides an exact position of the end-point within one period of $P=100\mu\text{m}$. Since the detected phase does not provide a coordinate of the end-point of the cylinder along the x-axis, the phase distribution of the SVIP whose x-coordinates are given by the positions of the CCD pixels is used as a scale with a high resolution of $P/100$. The coordinate of the end-point is obtained by assigning a value of the scale to the phase detected at the end-point in the sectional image. The obtained two positions of the end-points lead to the external diameter of the cylinder. It is shown that the method using the SVIP and the positions of the CCD pixels is useful for measuring diameters of metal cylinders.

2. PRINCIPLE

A configuration of setup for measuring an external diameter of metal cylinder is shown in Fig.1. The output light beam from a laser diode (LD) is collimated by lens L1 and divided into two beams by a beam splitter (BS). The two beams are reflected by two mirrors M1 and M2, respectively. The reflected lights from the mirrors M1 and M2 pass through the beam splitter and are combined together again. By adjusting the inclinations of the two mirrors M1 or M2, an interference fringe pattern of period P parallel to y-axis is obtained. The collimated laser beams forming the interference pattern enter an afocal imaging system which consists of lenses L2 and L3. On the spectral plane of this afocal imaging system, mask MA1 with two pinholes eliminates undesirable lights for the formation of the interference pattern. The interference pattern with an exact sinusoidal intensity distribution is obtained and projected

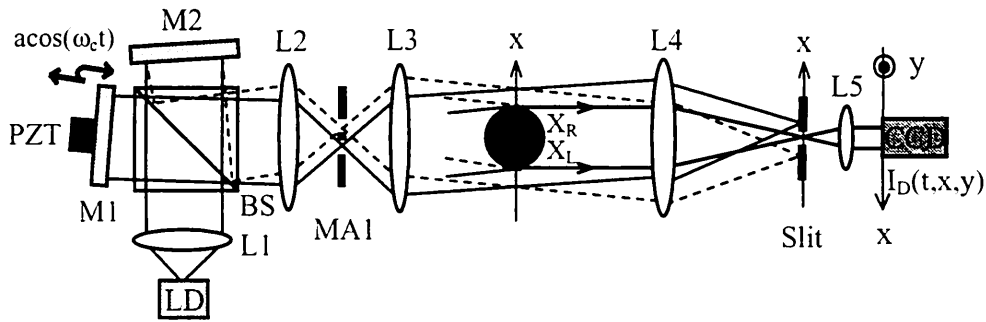


Fig.1 Configuration of an instrument for measuring external diameter of metal cylinders.

on the surface of a metal cylinder. Assuming that the intensity of the two beams and the visibility of the fringes are unity for the sake of simplicity, the sinusoidal intensity distribution on the x-y plane where an object is placed is expressed by

$$I(x, y) = 1 + \cos\left(\frac{2\pi}{P}x\right). \quad (1)$$

where P is the period of the interference pattern.

When the mirror M1 is vibrated by piezoelectric transducer (PZT) with a sinusoidal waveform of $\text{acos}(\omega_c t)$, the interference pattern is sinusoidally vibrated along the x-axis. This sinusoidally vibrating interference pattern (SVIP) is expressed by

$$I(t, x, y) = 1 + \cos\left[Z \cos(\omega_c t) + \frac{2\pi}{P}x\right], \quad (2)$$

where

$$Z = \frac{2\pi}{P}a. \quad (3)$$

Positions of end-points of the metal cylinder are denoted by X_L and X_R as shown in Fig.1. The surface of the metal cylinder diffracts and reflects the two beams forming the SVIP. An afocal imaging system which consists of lenses L4 and L5 is used to form a cross sectional image of the metal cylinder. A slit is put on the spectral plane c the afocal imaging system to select the lights only coming from the end-points of the metal cylinder. The intensity distribution on the cross sectional image in the image plane is expressed by

$$I_D(t, x, y) = A(x, y) + B(x, y) \cos\left[Z \cos(\omega_c t) + \alpha(x, y)\right]. \quad (4)$$

where $A(x, y)$, $B(x, y)$, and $\alpha(x, y)$ depend on the object and the shape of the slit. The time-varying intensity $I_D(t, x,$

y) is the same as the interference signal produced in sinusoidal phase-modulating (SPM) interferometer.^{7,8} $I_D(t, x, y)$ detected with a CCD image sensor is processed in a computer with the method of SPM interferometry to obtain $B(x, y)$ and $\alpha(x, y)$.

Figure 2 shows how to measure the external diameter of the metal cylinder. The external diameter of the metal cylinder is D and x -coordinates of the two end-points are X_L and X_R . The cross sectional image presents the end-points on left side and right side of the metal cylinder. For the sake of simplicity, the left side of the cross sectional image is considered to obtain coordinate X_L of the end point. On the left side of the metal cylinder, the amplitude distribution $B(x, y)$ has a maximum value on a pixel of CCD image sensor whose number I_X along x -axis is N_L . Since the lights forming the image come from the end-point of the metal cylinder, the phase distribution $\alpha(x, y)$ varies very slightly along x -axis. Phase α_L detected at the maximum value of $B(x, y)$ provides an exact position of left side end-point within the region of one period P around $I_X=N_L$. To determine the coordinate of X_L , phase distribution of SVIP around the pixel of $I_X=N_L$ is detected. Phase α_{L1} in the phase distribution of SVIP is larger than α_L and nearest to α_L is selected. The selected phase α_{L1} is detected at the pixel of $I_X=N_{L1}$. The phase detected at the pixel of $I_X=N_{L1}+1$ is denoted by α_{L2} , where the condition of $\alpha_{L2} \leq \alpha_L \leq \alpha_{L1}$ is satisfied. Since the interval of the adjacent pixels is known as ΔX , the position of left side end-point is given by

$$X_L = N_{L1}\Delta X + \frac{\alpha_{L1} - \alpha_L}{\alpha_{L1} - \alpha_{L2}} \Delta X \quad (5)$$

In the same ways phases $\alpha_R, \alpha_{R1}, \alpha_{R2}$ and N_{R1} are detected on the right side of the cross sectional image, and the position of right side end-point is given by

$$X_R = N_{R1}\Delta X + \frac{\alpha_{R1} - \alpha_R}{\alpha_{R1} - \alpha_{R2}} \Delta X \quad (6)$$

The external diameter is obtained as $D=X_R-X_L$.

In Secs.4 and 5, experimental results will show in details how to measure diameters of metal cylinders from amplitude distribution $B(x, y)$, phase distribution $\alpha(x, y)$, and the phase distribution of the SVIP.

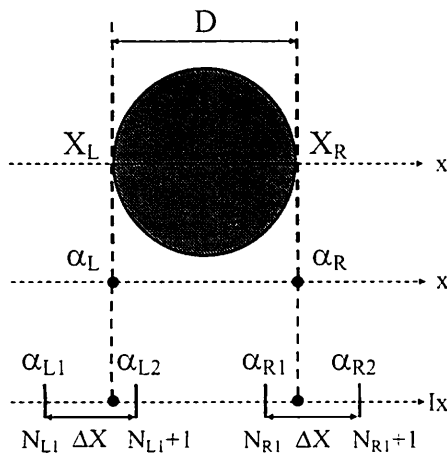


Fig. 2 Relations among the diameter and the measured values.

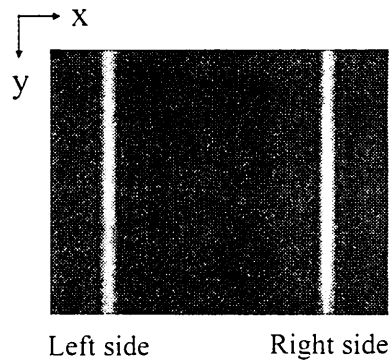


Fig. 3 Cross sectional image of the metal cylinder.

3. EXPERIMENTAL SETUP

The instrument shown in Fig.1 was constructed. The power of the laser diode (LD) was 30mW. Wavelength λ of the LD was 660nm. The period P of the interference pattern was $100\mu\text{m}$. Lenses L2 and L3 have the same focal length of 100mm. The diameter of the two pinholes used in mask MA1 was $200\mu\text{m}$. The sinusoidal vibrating frequency $\omega_c/2\pi$ was 177Hz. The external diameters of the metal cylinders were 9mm and 8mm. The focal length of the lenses L4 and L5 were 150mm and 50mm, respectively. The width of the slit was $200\mu\text{m}$. The magnification M of the afocal imaging system was about 1/3. Number of CCD pixels was 1024×768 , and the pixel size of CCD was $4.65\mu\text{m} \times 4.65\mu\text{m}$. A feedback control system to eliminate effect of external disturbances kept the phase distribution of the SVIP constant with time.⁹

4. MEASUREMENT OF PHASES ON THE END-POINTS

When the SVIP was projected onto the surface of the metal cylinder, in the spectrum plane of the lens L4 the slit was put on the middle position between the two spectrums of the two incident beams whose propagation direction did not change. The cross sectional image of the metal cylinder is shown in Fig.3. The size of the image was about 14mm and 10mm on the object along x-axis and y-axis, respectively. This picture was taken when the mirror M1 did not vibrate. When the mirror M1 was vibrated, the time-varying intensity $I_D(t, x, y)$ was detected with the CCD image sensor.

The amplitude distribution $B(x, y)$ and the phase distribution $\alpha(x, y)$ detected on the left side and right side of the cross sectional image at the y-coordinate of 2.8mm were shown in Figs.4 and 5, respectively. The amplitude distribution $B(x, y)$ had one peak and a maximum value at the pixel of $I_X=160$ as shown in Fig.4 (a). The phase distribution $\alpha(x, y)$ varied very slightly along x-axis as shown in Fig.4 (b). The phase detected at the maximum value of the amplitude distribution $B(x, y)$ was denoted by α_L as shown in Fig.4 (b). In the same way, phase α_R was detected at the pixel of $I_X=807$ as shown in Fig.5 (b).

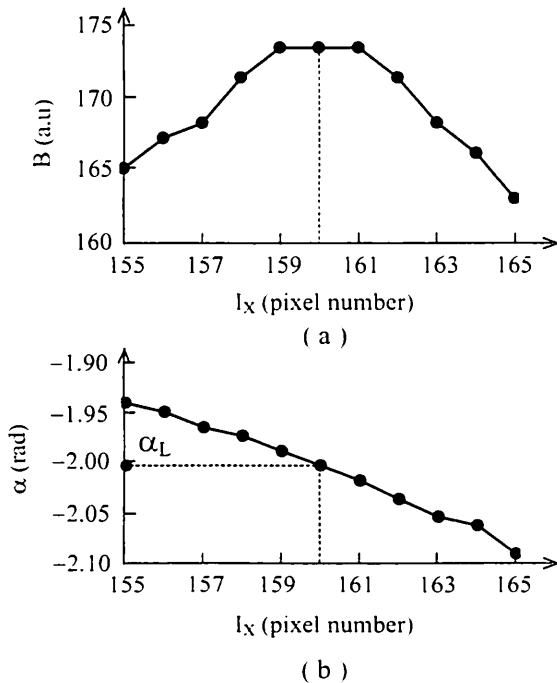


Fig. 4 Measurement of phase α_L of the left end-point at $y=2.8\text{mm}$. (a) Amplitude B . (b) Phase α of the image along x-axis.

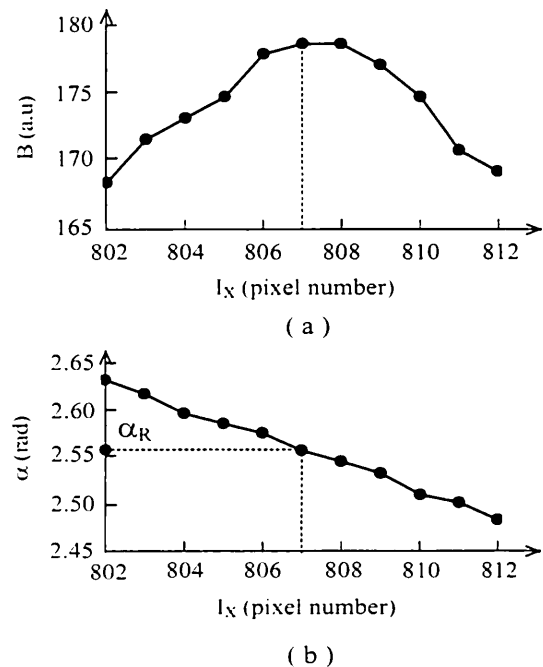


Fig. 5 Measurement of phase α_R of the right end-point at $y=2.8\text{mm}$. (a) Amplitude B . (b) Phase α of the image along x-axis.

When there were uncertainties in determination of the maximum value of the amplitude $B(x, y)$, these uncertainties caused the measurement error. The smaller phase difference between adjacent pixels provided a smaller error. In addition, the smaller phase difference provided a larger interval of the measuring points or a larger measurement region. When the slit of $200\mu\text{m}$ -width was used, the phase difference of two adjacent pixels was less than 0.02 rad as shown in Figs.4 (b) and 5 (b). This small phase difference corresponded to a measurement error of $0.3\mu\text{m}$ at $P=100\mu\text{m}$. The interval of measuring point was about $P/7=14\mu\text{m}$, and the measurement region was $14\text{mm}\times 10\text{mm}$ with the CCD pixel number of 1024×768 .

5. POSITIONS DETERMINATIONS OF THE END-POINTS

Figure 6 (a) shows the detected phase distributions of α_{L1} , α_L , and α_{L2} along the y-axis. The phase α_{L1} was detected at $N_{L1}=157$ along the x-axis. Figure 6 (b) shows the position X_L of the left end-point calculated with Eq.(5). Angle of the inclination of the least squares approximate line of the position X_L was 0.0004rad . Figure 7 (a) shows the detected phase distributions of α_{R1} , α_R , and α_{R2} . The phase α_{R1} was detected at $N_{R1}=802$. The position X_R of the right end-point was calculated with Eq.(6). The result is shown in Fig.7 (b), where angle of the inclination of the positions X_R was also 0.0004rad . The external diameter of $D=X_R-X_L$ was obtained. The external diameter of the metal cylinder was known as 9mm with a high accuracy. The ratio of the measured value and the known value of the diameter provided the exact magnification M of the imaging system. The diameter modified by the exact magnification is shown in Fig.8. Next a metal cylinder of 8mm -diameter was measured and the measured result is shown in Fig.9. These two measured values of the external diameters have variations of magnitude of $\pm 2\mu\text{m}$ along the x-axis.

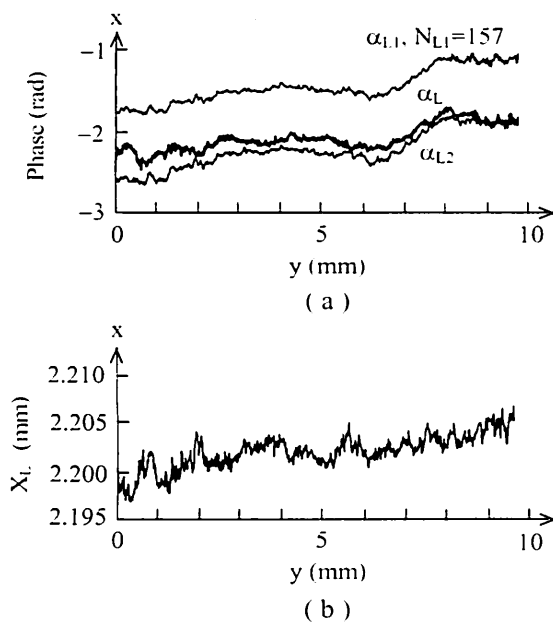


Fig. 6 Measurement of the coordinate of the left end-point. (a) Phase distributions α_{L1} , α_L , and α_{L2} . (b) Position X_L along the y-axis.

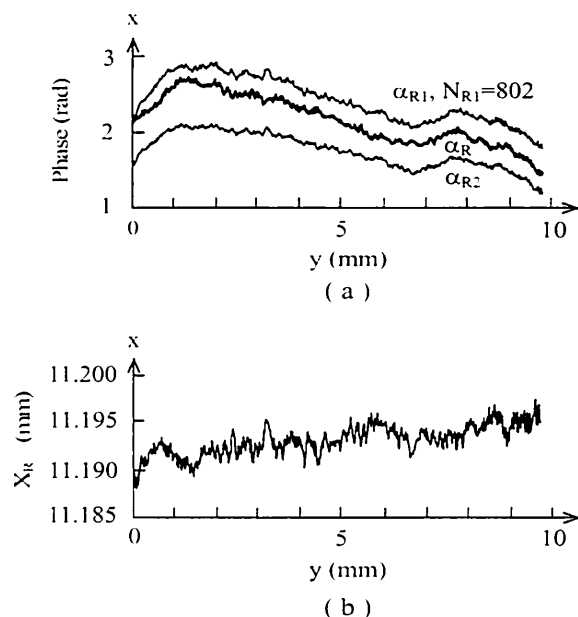


Fig. 7 Measurement of the coordinate of the right end-point. (a) Phase distributions α_{R1} , α_R , and α_{R2} . (b) Position X_R along the y-axis.

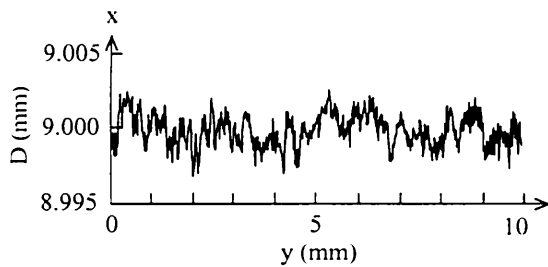


Fig. 8 Measured values of 9mm-diameter of the metal cylinder.

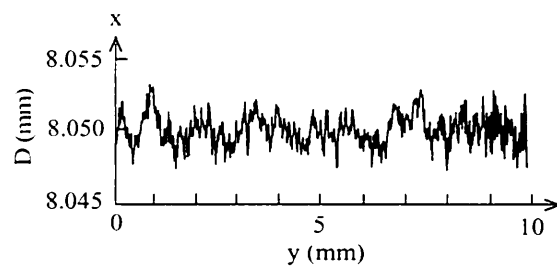


Fig. 9 Measured values of 8mm-diameter of the metal cylinder.

6. CONCLUSION

A method for measuring external diameters of metal cylinders was proposed, where the SVIP was used as an exact scale of the phase distribution. The lights from the end-points of the metal cylinder were extracted by a slit to form the cross sectional image of the metal cylinder. On the image the sinusoidally phase-modulated signal was detected and the phases of two end-points of the cylinder were measured. The coordinates of the two end-points were calculated from the phases of the two end-points and the phase distributions of the SVIP, which led to the external diameter. Metal cylinders of 9mm and 8mm-diameters were measured, where the measured values of the diameters had variations of magnitude of $\pm 2\mu\text{m}$.

REFERENCES

1. W Tang, Y Zhou and J Zhang, "Improvement on theoretical model for thin-wire and slot measurement by optical diffraction," *Meas. Sci. Technol.* **10**, N119-N123 (1999).
2. S. A. Khodier, "Measurement of wire diameter by optical diffraction," *Optics & Laser Technology* **36**, 63-67 (2004).
3. Dobosz M, "Measurement of fiber diameter using an edge diode beam of light," *Opt Commun* **58**(3), 172-176 (1986).
4. D. A. Cohen, "Calibration System Description: Model TRD-1 Outside Diameter Measurement System," Laser Metric, Inc. Calibration System Description (ANSI-Z540-1 1994), <http://laser-metric-systems.com/document>.
5. O. Sasaki, K. Hashimoto, Y. Fujimori, and T. Suzuki, "Measurement of cylinder diameter by using sinusoidally vibrating sinusoidal gratings," *Proc. SPIE* **4416**, 34-38 (2001).
6. J. Li, O. Sasaki, and T. Suzuki, "Measurement of sectional profile of a cylinder using a sinusoidally vibrating light with sinusoidal intensity," *Opt. Rev.* **9**, 159-162 (2002).
7. O. Sasaki and H. Okazaki, "Sinusoidal phase modulating interferometry for surface profile measurement," *Appl. Opt.* **25**, 3137-3140 (1986).
8. O. Sasaki, Y. Ikeda and T. Suzuki, "Superluminescent diode interferometer using sinusoidal phase modulation for step-profile measurement," *Appl. Opt.* **37**, 5126-5131 (1998).
9. O. Sasaki, K. Takahashi, and T. Suzuki, "Sinusoidal phase modulating laser diode interferometer with a feedback-control system to eliminate external disturbance," *Opt. Eng.* **29**, 1511-1515 (1990).